Scientific Research Publishing

Journal of Geoscience and Environment Protection, 2023, 11, 52-63
https://www.scirp.org/journal/gep
ISSN Online: 2327-4344
ISSN Print: 2327-4336

Land Surface Temperature Change in Hangzhou Urban Area in Recent 20 Years Based on Landsat Image

Siyi Wu

College of Geography and Environmental Sciences, Zhejiang Normal University, Jinhua, China
Email: 609305939@qq.com

How to cite this paper: Wu, S. Y. (2023). Land Surface Temperature Change in Hangzhou Urban Area in Recent 20 Years Based on Landsat Image. *Journal of Geoscience and Environment Protection, 11,* 52-63.
https://doi.org/10.4236/gep.2023.114005

Received: February 23, 2023
Accepted: April 25, 2023
Published: April 28, 2023

Abstract

Since the reform and opening-up in 1978, the urbanization level of our country has been continuously improved and the urban development has made great progress. However, with the rapid expansion of urban construction land, the population density and building density have been greatly increased, resulting in the urban heat island effect, which has negative impact on the urban thermal environment and restricts the high-quality development of urbanization. This paper focuses on how the urban surface thermal environment of Hangzhou changes in 20 years. In this paper, the characteristics of land surface temperature (LST) in Hangzhou urban area from 2000 to 2020 were studied by using Landsat images. The radiative transfer equation method is used to retrieve the land surface temperature, and the retrieval results are analyzed. The results show that: 1) the land surface temperature in Hangzhou city area has a slight upward trend in the past 20 years; 2) the area of high temperature area is expanding; 3) the land surface temperature in the city center area has decreased significantly in the past 20 years, while the ground temperature in other areas around the city center has increased significantly.

Keywords

Land Surface Temperature, Atmospheric Correction Method, Hangzhou, Landsat

1. Introduction

According to the sixth assessment report of the Intergovernmental Panel on Climate Change (IPCC), the global average temperature is 1.09˚C higher than the pre-industrial level due to the excessive dependence of human activities on

fossil fuels. As the interface of energy exchange between the earth and atmosphere, the change of air temperature will inevitably cause the change of soil temperature. In fact, the change of soil temperature is a response of soil thermal state to long-term climate change.

Land surface temperature (LST) is a key factor affecting the interaction between the atmosphere and water cycle, and is also an important parameter for the study of land surface energy balance and its dynamic change, has been widely applied to the researches of urban heat island effect, drought monitoring, climate change and the like, the urban land surface thermal environment is one of the manifestations of the urban thermal environment, reflects the urban land surface thermal environment, generally takes the land surface temperature as a measurement index, researches on the urban land surface temperature are carried out, and the research has important significance for understanding the change of the relationship between climate factors and urban soil surface characteristics, further understanding the change of urban soil surface air temperature and the interaction mechanism between the urban soil surface air temperature and environment-related variables and the like, has great scientific research value.

The main research area of this paper is Hangzhou City, which is located between 29˚11' - 30˚34' N and 118˚20' - 120˚37'E. It is the capital of Zhejiang Province and one of the central cities in the Yangtze River Delta. The city has 10 municipal districts, 2 counties and 1 county-level city under its jurisdiction, with a total area of 16,850 square kilometers.

With the continuous development of China, the urbanization level of our country has improved significantly, so does Hangzhou. Since 2000, the urbanization level has been continuously developing, rising rapidly from 36.52% to 75.30% in 2019, showing an accelerating trend. According to the famous "Northam curve," Hangzhou City urbanization level as early as 2011 (the urbanization rate of 71.11%) has entered the third stage of urbanization process-late mature stable stage. Hangzhou's urbanization spatial layout has been continuously optimized, and the quality of new urbanization has been steadily improved. The rapid expansion of urban construction land and the improvement of supporting facilities provide a large number of jobs, but at the same time, rapid urbanization is accompanied by the change of urban physical space environment and its negative impact.

2. Related Works

The main research data of atmospheric thermal environment is meteorological data, and the main research data of surface thermal environment is remote sensing data. Compared with atmospheric thermal environment, surface thermal environment is closely related to human perception and health, and can better reflect human activities (Ye et al. 2011; Wu & Chen, 2016). The concept of heat island effect recognized by academic circles was first proposed in 1833. United

Kingdom meteorologist Howard (Pedgley, 2003) found that the temperature in London Urban area was higher than that in the outer suburbs through 30-year temperature monitoring of London. Since then, the study of urban thermal environment using temperature data has been gradually carried out abroad.

1972, Rao (Rao, 1972) it is the first time in the world to use remote sensing to study the thermal environment of the earth's surface, and accordingly completed the paper "Detecting Urban Heat Island Effect by Environmental Satellite." Since then, a variety of sensors have been used to detect the thermal environment of the earth's surface. In 1978, the American Thermal Inertia Satellite (HCMM) was launched into space, which marked the beginning of the development of thermal infrared remote sensing. Thermal infrared remote sensing has many advantages, such as wide coverage, good time synchronization, rich data sources, etc. These characteristics make up for the shortcomings of traditional weather station measurement, which is also the reason why the application of remote sensing technology is more and more popular in recent years. So far, the retrieval of land surface temperature from thermal infrared remote sensing is one of the most commonly used methods.

Price et al. (Price, 1984) were the first to extend the method of retrieving sea surface temperature to land surface. Wan and Li (Wan & Li, 1997) obtained land surface temperature and land surface emissivity based on MODIS data by using multi-spectral band method. Yesihrmak (Yesihrmak, 2013) found that the change of air temperature must cause the change of land surface temperature, that is, the main leading effect of air temperature on land surface temperature is very obvious. Chichirez et al. (Chichirez et al., 2013) found that in some cities of Romania, the surface temperature has a similar trend to the air temperature, especially in winter and summer of the year.

The research on urban thermal environment in China started late, but made rapid progress, especially the launch of China-Brazil Earth Resources Satellite for observing land resource changes and monitoring man-made and natural disasters developed by China in 1999 greatly enriched the data sources for urban thermal environment research (Zhang et al., 2006; Zhou et al., 2007). The research on land surface thermal environment mainly focuses on algorithm research, urban heat island and regional land surface thermal environment research.

In a paper published in 2001, Qin Zhihao and other scholars (Qin et al., 2001) gave a single-window algorithm based on the surface radiative transfer equation, which effectively avoided the dependence of the radiative transfer equation calculation method on the real-time atmospheric profile. Based on this calculation method, only three data-atmospheric transmittance, atmospheric average acting temperature and surface emissivity are needed to achieve a better inversion effect. In addition, other algorithms have been continuously proposed. For example, Liu Zhiwu et al. (Liu et al., 2003) proposed an algorithm for retrieving land surface temperature according to ASTER remote sensing data source. Zhang Xiaofei et al. (Zhang et al., 2006) quantitatively analyzed the relationship be-

tween land surface temperature and vegetation cover in Shenzhen by using ETM+ images in 2004. Chen Yunhao et al. (Chen et al., 2002) made fractal calculation by using three aspects of thermal field structure in their research area-surface fractal, curve fractal and pixel point analysis, thus explaining the distribution of land surface temperature in their research area.

At present, the study of land surface temperature is not only limited to the urban heat island effect, but also extended to the research field of climate and ecological environment.

3. Data and Methods

3.1. Research Data and Research Process

This paper mainly uses geospatial data cloud and USGS website (https://earthexplorer.usgs.gov/), vector maps of all administrative regions in Zhejiang Province, atmospheric transmittance, atmospheric up-and down-going radiation, etc., the land surface temperature distribution map of Hangzhou urban area is obtained, and the trend analysis of land surface temperature change for many years is carried out. The main process is shown in **Figure 1**.

1) Download data and preprocessing

First, download the data of Hangzhou city from the website, and use the vector administrative map of Zhejiang Province at all levels as auxiliary data to do cutting processing and subsequent analysis. All data were projected uniformly to WGS-1984-UTM-Zone-51N during data preprocessing. Preprocessing mainly includes radiometric calibration, atmospheric correction, clipping and so on.

2) Modeling

The necessary data are obtained respectively, the vegetation coverage is obtained from the NDVI value, and then the specific emissivity is calculated; the blackbody radiation brightness value is calculated by combining the data such as the atmospheric transmittance and the like, and the land surface temperature inversion model is established according to the blackbody radiation brightness value.

3) Land surface temperature distribution map and analysis

Carry out trend analysis on the land surface temperature for many years to obtain the trend change map. In combination with the land surface temperature distribution map, analyze and discuss different regions, explore the causes of temperature distribution and change, and form the final conclusion.

3.2. Research Methods

1) Normalized Difference Vegetation Index

The normalized difference vegetation index (NDVI) is the ratio of the difference between the near-infrared band and the visible band to the sum of the two bands.

$$\mathrm{NDVI} = \frac{\rho_{nir} - \rho_r}{\rho_{nir} + \rho_r} \tag{1}$$

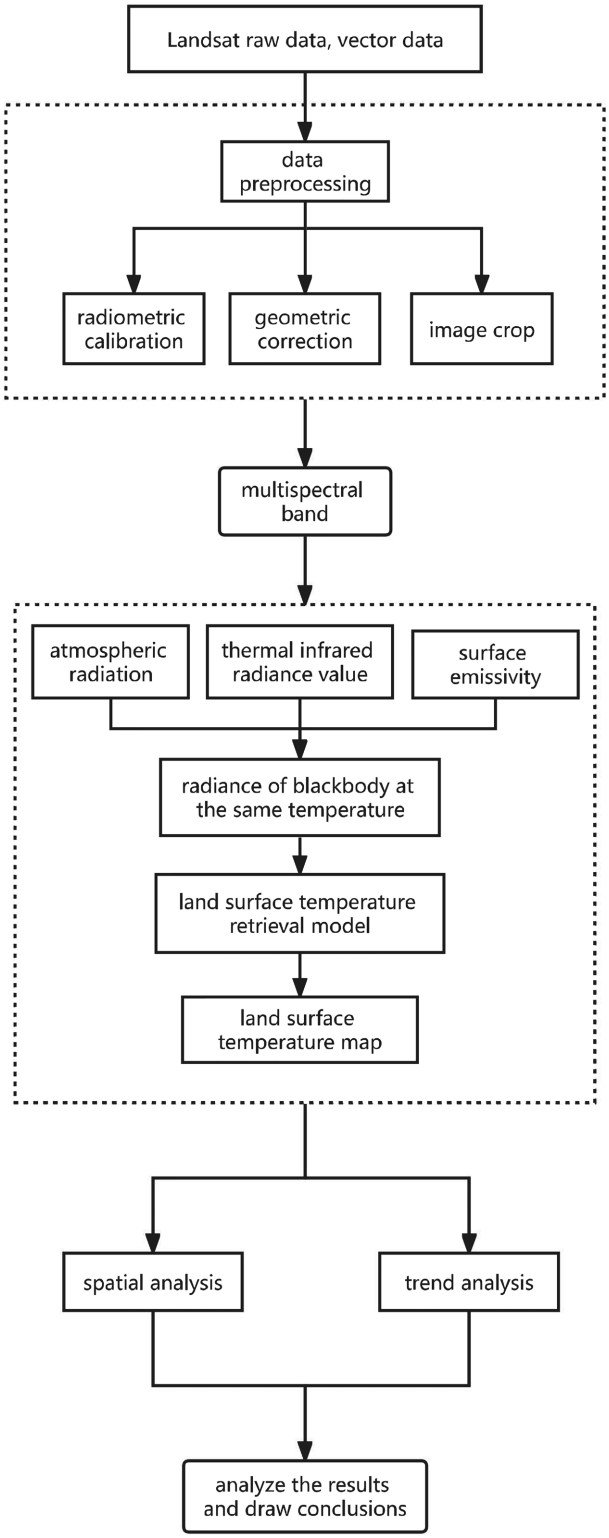

Figure 1. Study flow chart.

In the formula, ρ_{nir} represents the near-infrared band, and ρ_r represents the infrared band.

2) Vegetation Coverage

Vegetation Coverage (FVC) represents the percentage of the vertical projection area of vegetation on the ground to the total area of the study area. The formula is as follows.

$$\mathrm{FVC} = \frac{\mathrm{NDVI} - \mathrm{NDVI}_{\mathrm{soil}}}{\mathrm{NDVI}_{\mathrm{veg}} - \mathrm{NDVI}_{\mathrm{soil}}} \tag{2}$$

In the formula, $\mathrm{NDVI}_{\mathrm{soil}}$ is the NDVI value of bare soil or no vegetation coverage area, and $\mathrm{NDVI}_{\mathrm{Veg}}$ represents the NDVI value of the pixel completely covered by vegetation, i.e. the NDVI value of the pixel with pure vegetation. Take the empirical values $\mathrm{NDVI}_{\mathrm{Veg}} = 0.70$ and $\mathrm{NDVI}_{\mathrm{soil}} = 0.05$.

3) Emissivity

Emissivity is the ratio of the radiant exitance of an object at temperature T and wavelength λ to the radiant exitance of a blackbody at the same temperature and wavelength. In this study, the NDVI threshold method proposed by Sobrino (Liu et al., 2012) was used. In BandMath, input the surface emissivity formula according to the requirements, and calculate the surface emissivity image according to the vegetation coverage.

$$\varepsilon = 0.004\mathrm{FVC} + 0.986 \tag{3}$$

4) Blackbody radiance

Radiance $B(T_S)$ of Blackbody at Temperature T in Thermal Infrared Band.

$$B\left(T_S\right) = \frac{\left[L_\lambda - L\uparrow - \tau\left(1-\varepsilon\right)L\downarrow\right]}{\tau\varepsilon} \tag{4}$$

where ε is the surface emissivity; T_s is the true surface temperature (K); $B(T_s)$ is blackbody thermal radiance; τ is the transmittance of atmosphere in thermal infrared band.

5) Unitary linear regression method and significance test

$$y = ax + b$$

$$\mathrm{slope} = \frac{n\sum_{i=1}^{n}\left(i \times \mathrm{NDVI}_i\right) - \sum_{i=1}^{n} i \times \sum_{i=1}^{n} \mathrm{NDVI}_i}{n\sum_{i=1}^{n} i^2 - \left(\sum_{i=1}^{n} i\right)^2} \tag{5}$$

n refers to the number of years of detection, i refers to the year of detection, NDVI_i refers to the observed NDVI value of the ith year, slope refers to the gradient of change, i.e. slope, and its value can be positive or negative: Positive values indicate an increasing trend with time, and the greater the value, the more obvious the increasing trend; Negative values indicate a decreasing trend over time, and the greater the absolute value, the more significant the decreasing trend.

$$\begin{aligned} b &= \overline{y} - a\overline{x} \\ F &= \frac{U}{Q/(n-2)} \\ U &= b^2\sum_{i=1}^{n}\left(x_i - \overline{x}\right)^2 \\ Q &= \sum_{i=1}^{n}\left(y_i - y'\right) \end{aligned} \tag{6}$$

The significance test is conducted by F test method (Formula 6). $\overline{Y}$ is the average annual value of NDVI, $\overline{X}$ is the mean value of the year, and y' is the fitting value obtained after fitting the unitary linear model. F is the significance test value, and its significance can be obtained by looking up the table.

6) Classification

See Table 1 for classification criteria of surface temperature.

4. Using the Template

4.1. Annual Mean Land Surface Temperature

The annual mean value of the land surface temperature from 2000 to 2020 is calculated, and the results are shown in Table 2.

The annual average land surface temperature is made into a line chart, and the result are shown in Figure 2.

It can be seen from Figure 2 that the highest annual surface temperature is 40.98˚C in 2003; The lowest annual surface temperature was 23.59˚C in 2005.

4.2. Spatio-Temporal Analysis

4.2.1. Time (Trend) Analysis

In the classic version of ENVI trend analysis plug-in trend analysis. Generally,

Table 1. Classification criteria of land surface temperature.

Grading Standard	Surface Temperature Class
$\mu + SD \leq T_i$	High temperature region (HT)
$\mu + 0.5SD \leq T_i < \mu + SD$	Secondary high temperature region (SHT)
$\mu - 0.5SD \leq T_i < \mu + 0.5SD$	Middle temperature region (MT)
$\mu - SD \leq T_i < \mu - 0.5SD$	Secondary low temperature region (SLT)
$T_i < \mu - SD$	Low temperature region (LT)

Table 2. Average land surface temperature Hangzhou City from 2000 to 2020.

Year	Mean (˚C)	Year	Mean (˚C)
2000	27.04	2011	20.77
2001	26.24	2012	27.79
2002	37.91	2013	38.89
2003	40.98	2014	25.73
2004	24.89	2015	23.85
2005	23.59	2016	33.82
2006	29.78	2017	31.92
2007	35.15	2018	19.17
2008	32.63	2019	28.61
2009	34.13	2020	35.2
2010	39.58		

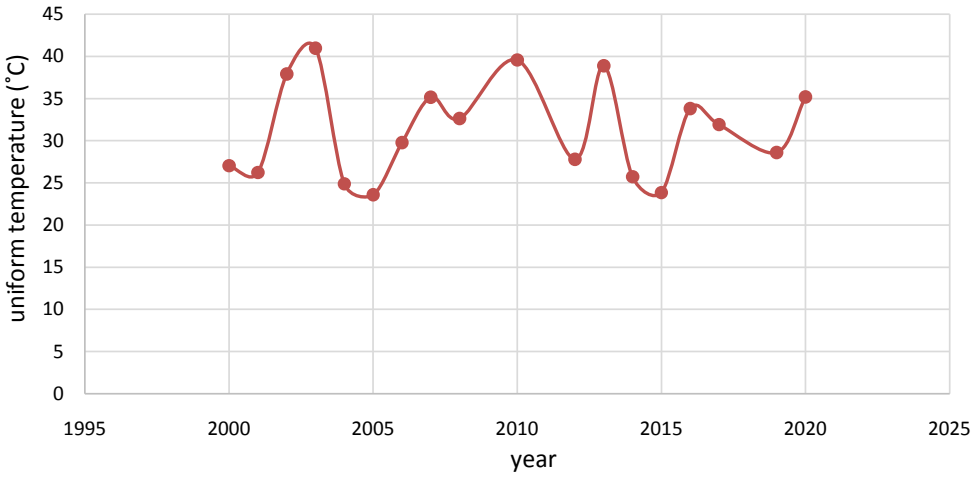

Figure 2. Average land surface temperature Hangzhou.

we divide June, July and August as summer. As some years deviate from summer, the trend analysis will be conducted after excluding them, and the precision will be higher.

From **Figure 3**, we can see that, on the whole, there is a linear correlation between the year and the temperature, and it is a positive correlation, indicating that the surface temperature of the municipal district of Hangzhou in the past 20 years has shown a slight upward trend.

4.2.2. Spatial Analysis

According to the mean-standard deviation classification method, we divide the land surface temperature into five grades, which are low temperature, sub-low temperature, medium temperature, sub-high temperature and high temperature in turn. By using the reclassification method, we calculate the area of different graded temperature areas by using the method of table grid display partition statistics in ArcGIS, the result are shown in **Table 3** and **Figure 4**.

Longitudinal comparison shows that there are different degrees of area change in each temperature zone. Among them, the area of low temperature area has expanded in recent years, but there is a downward trend. The area of sub-low temperature area has an upward trend, the area of medium temperature area has a slow downward trend, the area of sub-high temperature area has increased in different degrees in recent years, but has a downward trend, and the area of high temperature area will continue to expand.

Horizontal comparison shows that the area proportion of medium temperature area is the largest Hangzhou City every year, followed by the second low temperature area and low temperature area. Basically, from 2010, the second high temperature area and high temperature area gradually occupy the upper hand and replace the position of the second low temperature area and low temperature area.

In terms of amplitude, the medium temperature zone and the second low temperature zone have larger amplitude.

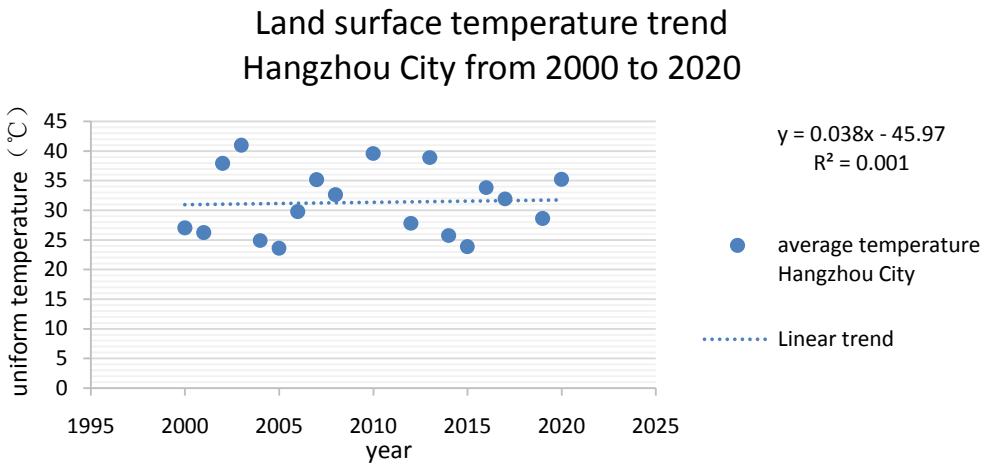

Figure 3. Land surface temperature trend Hangzhou City.

Table 3. Change in area of graded temperature zone.

Year	LT (km²)	SLT (km²)	MT (km²)	SHT (km²)	MT (km²)
2000	438.4935	840.3903	1298.7792	512.4294	263.3124
2001	553.8546	297.0576	1817.2089	406.26	285.0219
2002	453.6891	569.322	1649.9817	342.5985	343.8126
2003	306.4563	1047.9654	1221.2154	401.4342	382.344
2004	594.8838	668.5443	1266.3819	455.9148	373.6809
2005	461.0349	394.9083	1830.3543	319.5936	353.5119
2006	758.1933	916.6635	1128.5946	203.8797	351.7002
2007	408.3975	1065.1725	1290.1671	266.7672	328.5279
2008	583.1019	432.6507	1572.0786	448.1775	323.0235
2009	549.1206	550.0899	1459.5795	428.2731	371.9691
2010	645.3819	937.6416	1019.1843	277.6617	479.1627
2011	479.4057	390.9141	1615.2687	475.3953	397.0116
2012	414.0612	488.0709	1504.8072	512.2386	438.4638
2013	516.1059	497.0259	1269.7488	491.8131	583.3053.
2014	347.8779.	381.6054	1696.1589	614.1033	318.2535
2015	469.9539	578.412	1406.8188	441.3051	461.5092
2016	374.6214	576.3681	1410.4179	532.7496	463.842
2017	444.7539	588.3264	1339.7679	512.703	472.4478
2018	484.3026	364.7952	1541.637	626.9859	340.2783
2019	508.9563	611.8704	1221.4314	519.6339	496.107
2020	543.6864	555.9741	1218.3723	504.0792	535.887

4.2.3. Extent of Change in Surface Temperature

The trend was tested for significance using the F-test. We divide the change trend into 4 levels according to the test results, as shown in **Figure 5**.

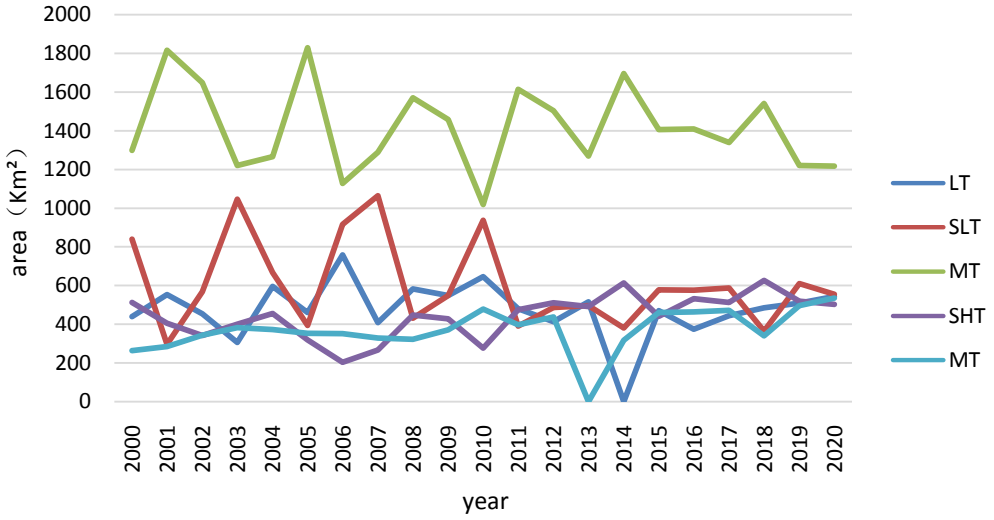

Figure 4. Example of a figure caption (figure caption).

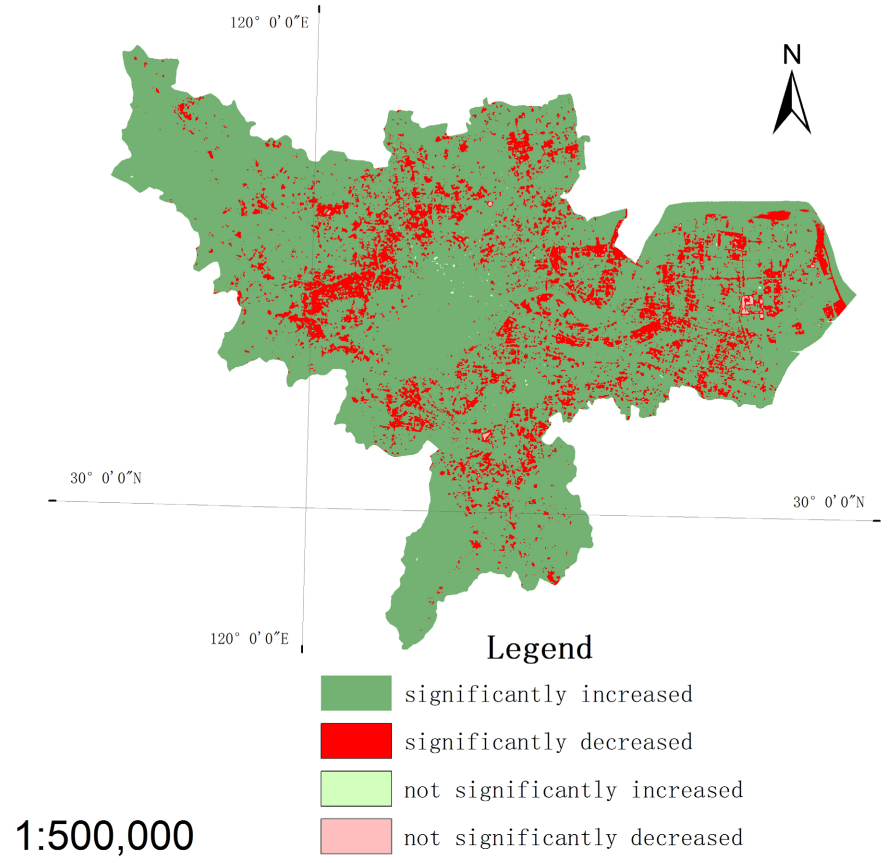

Figure 5. Extent of change in surface temperature.

As can be seen from the figure, the overall significant increase in area is less than the decrease in area. From the local point of view, the significant and non-significant reduction areas are mainly located in the core area of Hangzhou City, the south, northwest and scattered distribution in the vicinity of Qiantang River. The areas with significant increases are mainly located around the center

of Hangzhou.

The results show that the ecological construction of Hangzhou City has achieved some results. According to the grand blueprint for building a new ecological Qiantang proposed in the special ecological planning of Qiantang District in Hangzhou, explore the green and low-carbon development mode, build a comprehensive demonstration area for biological development, and create a template for the construction of new industrial areas with the concept of garden city. At the same time, the famous West Lake scenic spot in the center of Hangzhou City and some forest parks around it also play a role in regulating the ground temperature.

5. Conclusion

According to the analysis of the trend of the surface temperature, we can draw the conclusion that the area of the high temperature area is expanding, although the temperature of the urban area is high in general. The ecological construction in Hangzhou City has made some achievements. The land surface temperature in the downtown area has decreased significantly in the past 20 years, while the ground temperature in other areas around the downtown area has increased significantly.

Conflicts of Interest

The author declares no conflicts of interest regarding the publication of this paper.

References

Chen, Y. H., Li, X. B., Shi, P. J., & He, C. Y. (2002). Analysis of Spatial Pattern of Urban Thermal Environment in Shanghai. *Science of Geography, 3,* 317-323.

Chichirez, C. M., CImpeanu, M. S., & Marin, D. I. (2013). Variability of Soil Surface Temperature in the Campulung Muscel Depression (Arges-Romania). *Agrolife Scientific Journal, 2,* 52-57.

Liu, F., Wang, X. S., Xu, J. et al. (2012). Parameter Sensitivity Analysis of Surface Emissivity Inversion Based on NDVI Threshold Method. *Telesense Information, 27,* 3-12.

Liu, Z. W., Dang, A. R., Lei, Z. D., & Huang, Y. G. (2003). Algorithm and Application of Retrieving Land Surface Temperature from ASTER Remote Sensing Data. *Advances in Geographical Sciences, 5,* 507-514+544.

Pedgley, D. E. (2003). Luke Howard and His Clouds. *Weather, 58,* 51-55. https://doi.org/10.1256/wea.157.02

Price, J C. (1984). Land Surface Temperature Measurements from the Split Window Channels of the NOAA 7 Advanced Very High Resolution Radiometer. *Journal of Geophysical Research, 89,* 7231-7237. https://doi.org/10.1029/JD089iD05p07231

Qin, Z. H., Zhang, M. H., Arnon, K., & Pedro, B. (2001). A Single Window Algorithm for Calculating Surface Temperature Using Landsat TM6 Data. *Acta Geographica Sinica, 4,* 456-466.

Rao, P. K. (1972). Remote Sensing of Urban Heat Islands from an Environmental Satellite. *Bulletin of the American Meteorological Society, 53,* 647-648.

https://doi.org/10.1175/1520-0477-53.7.648

Wan, Z. M., & Li, Z. L. (1997). A Physics-Based Algorithm for Retrieving Land-Surface Emissivity and Temperature from EOS/MODIS Data. *IEEE Transactions Geoscience Remote Sensing, 35,* 980-996. https://doi.org/10.1109/36.602541

Wu, Z. F., & Chen, L. D. (2016). Thermal Comfort Evaluation and Urban Thermal Environment Research: Present Situation. Characteristics and Prospect. *Journal of Ecology, 35,* 1364-1371.

Ye, C. H., Liu, Y. H., Liu, W. D., Liu, C., & Quan, W. J. (2011). Research and Application of Remote Sensing Monitoring Indicators for Urban Surface Thermal Environment. *Meteorological Science and Technology, 39,* 95-101.

Yesihrmak, E. (2013). Soil Temperature Trends in Büyük Menderes Basin, Turkey. *Meteorological Applications, 21,* 859-866. https://doi.org/10.1002/met.1421

Zhang, X., Wang, Y., Wu, J., Li, W., & Li, Z. (2006). Quantitative Relationship between Land Surface Temperature and Vegetation Cover in Urban Area—A Case Study of Shenzhen. *Geographic Research, 3,* 369-377+561.

Zhang, Y., Gu, X. F., Yu, T., Zhang, Y. X., Qi, R. L., & Li, X. W. (2006). Cross Radiometric Calibration of Thermal Infrared Channels of CBERS. *Journal of Infrared and Millimeter Waves, 4,* 261-266.

Zhou, J., Zhao, D. L., He, Y. H., & Chen, J. (2007). Accuracy Evaluation of Land Use Classification Based on China-Brazil Satellite Image. *Science of Surveying and Mapping, 6,* 27-29+204.